Dielectric function of the electron gas with dynamical-exchange decoupling. II. Discussion and results*

F. Brosens and J. T. Devreese‡
Departement Natuurkunde, Universitaire Instelling Antwerpen, Universiteitsplein 1, B-2610 Wilrijk, Belgium
L. F. Lemmens
Institute of Applied Mathematics, Rijksuniversitair Centrum Antwerpen, Groenenborgerlaan 171, B-2020 Antwerpen, Belgium
(Received 16 February 1979; revised manuscript received 6 August 1979)

By making the dynamical-exchange decoupling in the equation of motion for the Wigner distribution function, exchange effects in the dielectric function of the homogeneous electron gas were, in an earlier derivation, described by a frequency-dependent local-field correction $G(q,\omega)$. In paper I, details were provided how the sixfold integral for $G(q,\omega)$ can be reduced analytically into a double integral, adapted for numerical purposes. In this paper, the consequences of dynamical-exchange effects are studied, and the theory is tested for its internal consistency. The evaluation of the pair correlation function $g(r)$ at the origin from both the static limit and the high-frequency limit of the frequency-dependent local-field correction $G(q,\omega)$ leads to the same value $g(0)=1/2$, in contrast to other theories where, from both limits, different results are obtained. Also, the compressibility, calculated from the dielectric function including exchange, agrees with the Hartree-Fock result. Furthermore, it is shown that the high-frequency limit of $G(q,\omega)$ satisfies the general properties implied by the third-frequency-moment sum rule, resulting again in $g(0)=1/2$ and leading to the Hartree-Fock ground-state energy. This consistency between the static and high-frequency behavior of $G(q,\omega)$ cannot be fulfilled by any static approximation to $G(q,\omega)$, because an adequate treatment of dynamical-exchange effects involves excited states that are consistent with the Hartree-Fock ground state. In the static limit, $G(q,\omega)$ exhibits a relatively sharp peak near $q=2k_F$. This peak induces an instability of the homogeneous electron gas, quite similar to and in the same density range as the instability of the spin susceptibility discussed by Hamann and Overhauser. For $r_s \geq 10.6$, a supplementary instability relative to charge-density deformations occurs. The frequency dependence of $G(q,\omega)$ is examined, and numerical values for $\mathrm{Re}G(q,\omega)$ and $\mathrm{Im}G(q,\omega)$ are presented. The real part of the dielectric function and the imaginary part of the inverse dielectric function are plotted for several densities in the metallic range. Compared to the random-phase approximation (RPA), the frequencies of the maxima in the structure factor obtained in the present work (i.e., with dynamical-exchange decoupling) are shifted to lower frequencies. The plasmon dispersion is considerably closer to recent experimental data in aluminium than with RPA. Finally, it turns out that the inclusion of frequency-dependent exchange effects results in the natural occurrence of spin- and charge-density waves. These are the dynamical extension of the instability relative to magnetic perturbations, found in the static limit at low densities.

I. INTRODUCTION

In Paper I,[1] the present authors studied an earlier-derived expression for the frequency-dependent local-field correction $G(q,\omega)$, which accounts for dynamical-exchange effects in the dielectric function $\epsilon(q,\omega)$ of jellium:

$$\epsilon(q,\omega)=1+Q_0(q,\omega)/[1-G(q,\omega)Q_0(q,\omega)], \quad (1)$$

where $Q_0(q,\omega)$ is the Lindhard polarizability. The local-field correction $G(q,\omega)$ depends not only on the wave vector, but also on the frequency in contrast to the local-field correction, introduced by Hubbard.[2] Paper I was merely devoted to reducing an explicit expression for $G(q,\omega)$ as a sixfold integral into a tractable double integral by analytical methods. To the best of our knowledge, this is the first detailed study and explicit evaluation of $G(q,\omega)$ at arbitrary frequency and wave vector. Some results for $\mathrm{Re}\epsilon(q,\omega)$ and $\mathrm{Im}\epsilon^{-1}(q,\omega)$ were displayed, and new analytical expressions for $G(q,\omega)$ were obobtained in some limiting cases.

In the present paper (Paper II), this study of the dynamical-exchange effects is continued. In Sec. II, the internal consistency of the dynamical-exchange-decoupling method and its relation to several sum rules is investigated. In Sec. III, the static limit of the dielectric function with dynamical-exchange decoupling is examined, and it is shown that an instability of the homogeneous paramagnetic state at low electron densities arises quite naturally. A similar instability was discussed previously by Hamann and Overhauser[3] in studying the spin susceptibility. In Sec. IV, a number of numerical results are presented. Furthermore, it is shown that the dynamical-exchange effects shift the frequencies of the maxima in the structure factor towards lower frequencies compared to the random-phase approximation (RPA). If exchange is included, the agreement with recent experimental data on the plasmon dispersion in aluminum[4] is substantially closer than in RPA. Finally, spin-density waves originate automatically from the dielectric function with dynamical-exchange effects.

II. CONSISTENCY REQUIREMENTS

In comparing theoretical predictions from the dielectric response function of the homogeneous electron gas to experimental results in metals, two fundamentally different sources for possible discrepancies can arise. The description of a metal with the jellium model, i.e., replacing the discrete lattice of atoms by a uniform neutralizing background, is an oversimplification. But even this simplified theoretical model is not exactly soluble, and several approximations have to be made within the framework of the model to derive the dielectric properties. The nature of the jellium model and the mathematical approximations made in the study of the model both influence the results, and comparison to the experiment does not provide a unique way to judge the validity of the theoretical assumptions. Therefore, exact interrelations among various quantities in the electron-gas model, which also can be calculated from the dielectric function, form a powerful tool for studying the consistency of the approximations made in deriving $\epsilon(q,\omega)$.

A. Static limit $\omega = 0$

In the static limit $\omega = 0$, the compressibility sum rule[5] relates the long-wavelength static dielectric function to the compressibility κ of the electron gas:

$$\epsilon(q,0) \underset{q\to 0}{\longrightarrow} 1 + (k_{\mathrm{FT}}{}^2/q^2)\kappa/\kappa_0 , \tag{2}$$

where k_{FT} is the Thomas-Fermi screening wave vector, and κ_0 is the compressibility of the noninteracting Fermi gas. The long-wavelength limit of the static local-field correction including dynamical exchange is given by[6-8]

$$G(q,0) \underset{q\to 0}{\longrightarrow} \tfrac{1}{4}(q/k_F)^2 . \tag{3}$$

This leads to

$$\epsilon(q,0) \underset{q\to 0}{\longrightarrow} \frac{4me^2}{\pi\hbar^2 k_F}\left(\frac{k_F}{q}\right)^2 \frac{1}{1-(r_s/\pi)(4/9\pi)^{1/3}} , \tag{4}$$

where r_s is the dimensionless Wigner-Seitz parameter. As is well known, the long-wavelength result (4) is also obtained by using in (2) the compressibility from the Hartree-Fock (HF) ground-state energy.

On the other hand, in the limit $q \to \infty$, one easily proves that, with dynamical-exchange decoupling,

$$G(q,0) \underset{q\to\infty}{\longrightarrow} \tfrac{1}{3} , \tag{5}$$

in agreement with the large-q limit of the first-order HF correction,[9] which is dominant at large q.

Furthermore, the pair correlation function $g(r)$ at the origin $r = 0$, is related to the large q limit of $G(q,0)$ by

$$G(q,0) \underset{q\to\infty}{\longrightarrow} \tfrac{2}{3}[1-g(0)] . \tag{6}$$

This is a rigorous relation for the electron gas, derived by Niklasson.[10] The limit (5) combined with (6) thus implies that $g(0) = \frac{1}{2}$ with dynamical-exchange decoupling. As is well known, the same result is also obtained from the static structure factor in the HF approximation.

The frequency-dependent approach to $G(q,\omega)$, worked out by Toigo and Woodruff[11] (hereafter referred to as TW), does not reproduce the large-q limit (5). This is discussed in detail in Ref. 12, where it is suggested that this discrepancy is due to an implicit averaging over all frequencies in the TW method.

The agreement between the HF approximation and the static limit of the dielectric function with dynamical-exchange effects in deriving the compressibility and the pair correlation function is to be expected, because, in the static limit, the dynamical-exchange decoupling reduces into the HF decoupling. This agreement simply indicates that the internal consistency of the decoupling method in the static limit is not disturbed by the variational procedure used to solve the equation of motion for the induced electron density.

B. High-frequency limit

An interesting consistency requirement, involving the high-frequency behavior of $\epsilon(q,\omega)$, can be derived from the work of Niklasson[10] and Kimball.[13] By noting that for a small interparticle separation the many-electron problem reduces to an effective two-body problem, these authors show that

$$g'(0) \equiv \left.\frac{dg(r)}{dr}\right|_{r=0} = \frac{1}{a_0} g(0) , \tag{7}$$

where a_0 is the Bohr radius.

The pair correlation function in terms of the static structure factor $S(q)$ is defined by

$$g(r) - 1 = \frac{1}{n}\frac{1}{(2\pi)^3}\int d^3q[S(q)-1]e^{i\vec{q}\cdot\vec{r}} , \tag{8}$$

where n is the electron density. From the properties of Fourier transforms, (8) leads to

$$g'(0) = -\frac{1}{8\pi n}\lim_{q\to\infty} q^4[S(q)-1] . \tag{9}$$

Combining (7) and (9), one deduces the Kimball-Niklasson relation

$$g(0) = -\frac{a_0}{8\pi n}\lim_{q\to\infty} q^4[S(q)-1] . \tag{10}$$

The fluctuation-dissipation theorem[14] relates the static structure factor to $\epsilon(q,\omega)$,

$$S(q) = -\frac{q^2}{4\pi e^2}\frac{\hbar}{n\pi}\int_0^\infty d\omega \,\mathrm{Im}\frac{1}{\epsilon(q,\omega)} , \tag{11}$$

and thus (10), combined with (11), allows one to calculate $g(0)$ from the frequency-dependent dielectric function in the long-wavelength limit.

On the other hand, in an independent way, $g(0)$ also follows from the static limit $G(q,0)$ by (6). Obtaining the same result from (6) and from (10)/(11) imposes severe conditions on the frequency dependence of $G(q,\omega)$. For instance, with any static approximation $G_s(q)$ for $G(q,\omega)$ used in the frequency-dependent dielectric function (1), (10)/(11) leads to[13]

$$\lim_{q\to\infty} G_s(q) = 1 - g(0)\,. \tag{12}$$

This relation (12), proposed by Shaw[15] from a static local-field model, thus neglects the dynamical-exchange and correlation effects, and is incompatible with the rigorous relation (6), except for $g(0)=1$, which from (7) would imply that $g(r)$ exceeds 1 near the origin. In order to satisfy (6) and (10)/(11) simultaneously, the frequency dependence in $G(q,\omega)$ has to be included explicitly. Any static approximation to $G(q,\omega)$ which differs from zero for $q\to\infty$ violates at least one of both conditions, as discussed in Ref. 16 for several specific cases.

For our dielectric function with dynamical-exchange decoupling, the integral (11) can be performed analytically in the limit $q\to\infty$. This derivation is given in the Appendix, and results in

$$\lim_{q\to\infty} q^4[S(q)-1] = -4\pi n/a_0\,. \tag{13}$$

We have already presented this result in Ref. 16 without derivation.

It should be noted that the frequency-dependent approximation by TW[11] also leads to the limiting behavior (13), and therefore $g(0)=\frac{1}{2}$ is also obtained from the high-frequency limit of their dielectric function by combining (10) and (13). At $\omega=0$, however, the TW local-field correction becomes $\frac{2}{3}$ (Ref. 12) in the large-q limit, and the static relation (6) then implies $g(0)=0$. With the TW approximation, one thus obtains a different value for $g(0)$ if derived from the static limit or from the high-frequency limit of $G(q,\omega)$. To the best of our knowledge, the dynamical-exchange-decoupling method presented here is the only method leading to the same value for $g(0)$ from both the conditions (6) and (10)/(11). More details are given in Ref. 16.

Another consistency requirement can be obtained from the third-frequency-moment sum rule, and the general analytical properties of $G(q,\omega)$ from which the following exact relations are derived[17]

$$G(q,\infty) \underset{q\to\infty}{\longrightarrow} -\frac{2q^2}{m\omega_p^2}\left(\langle E_k\rangle - \langle E_k\rangle_0 + \tfrac{2}{3}[1-g(0)]\right), \tag{14}$$

$$G(q,\infty) \underset{q\to 0}{\longrightarrow} -\frac{2q^2}{m\omega_p^2}\left(\langle E_k\rangle - \langle E_k\rangle_0 + \tfrac{2}{15}\langle V\rangle\right), \tag{15}$$

where $\langle V\rangle$ and $\langle E_k\rangle$ denote the average potential energy and the average kinetic energy per particle in the interacting electron gas, and where $\langle E_k\rangle_0$ is the average kinetic energy per particle in the noninteracting electron gas.

In Appendix A of Paper I, the high-frequency limit of $G(q,\omega)$ was derived, including dynamical-exchange effects. For large and small wave vector, respectively, the following expressions were obtained:

$$G(q,\infty) \underset{q\to\infty}{\longrightarrow} \tfrac{1}{3}[1 - \tfrac{4}{7}(k_F/q)^2 + \cdots]\,, \tag{16}$$

$$G(q,\infty) \underset{q\to 0}{\longrightarrow} \tfrac{3}{20}(q/k_F)^2 + \cdots\,. \tag{17}$$

Because (16) contains no term in q^2, (14) and (16) are only equivalent if the dielectric function (1) with dynamical-exchange decoupling implies that $\langle E_k\rangle = \langle E_k\rangle_0$. Comparing then (17) with (15), it follows that

$$\langle V\rangle = -\tfrac{9}{16}\, m\omega_p^2/k_F^2 = -(3/4\pi)e^2 k_F\,, \tag{18}$$

which is precisely the exchange energy in the HF approximation. Furthermore, the identification of the q-independent terms in (16) and (14) then again leads to $g(0)=\frac{1}{2}$, in agreement with the above results for the value of $g(0)$ obtained from the Niklasson relation (6) and the Kimball-Niklasson relation (10).

In summary, the static limit of the dielectric function obtained with the dynamical-exchange-decoupling method, presented in Paper I is consistent with the HF results for both the compressibility and the pair correlation function at the origin. *This is quite reasonable, because the HF approximation is the static limit of the dynamical-exchange decoupling.* Furthermore, as shown above, this dynamical-exchange treatment in the high-frequency limit is internally consistent with the static results for the energy and the pair correlation function, which gives confidence in the procedure used to solve the equation of motion for the Wigner distribution function. It is therefore not surprising that the dielectric function with dynamical-exchange decoupling conserves frequency moments to infinite order in the HF ground state as shown in Ref. 8 by an alternative derivation of the same formal expression for $G(q,\omega)$.

III. STATIC LIMIT OF $\epsilon(q,\omega)$ FROM DYNAMICAL-EXCHANGE DECOUPLING

From the two-dimensional integral for $G(q,\omega)$, given in Eq. (38) of Paper I, numerical values can be obtained by elementary numerical methods. Some results for $G(q,\omega)$ in the static limit $\omega=0$ have

been published previously.[18] In Fig. 1, $G(q,0)$ is plotted and compared to the local-field correction of other theories. $G(q,0)$ can also be obtained formally by considering the susceptibility from a diagrammatic expansion[9] as the first two terms in a geometric series in powers of e^2. A theoretical justification of this procedure is given in Ref. 18.

As discussed in the previous section, the behavior of $G(q,0)$ in the long-wavelength limit $q \to 0$ is given by (3), leading to the HF compressibility. With increasing q, $G(q,0)$ first increases until its maximum near $q = 2k_F$. For $q > 2k_F$, $G(q,0)$ decreases and smoothly reaches its asymptotic value $G(q,0) \to \frac{1}{3}$ (as $q \to \infty$), which leads to $g(0) = \frac{1}{2}$, as is consistent with the high-frequency limit of $G(q,\omega)$.

In the HF approximation, the electron gas is unstable for $r_s \geq 6.0292$, as reflected in the sign inversion of the compressibility modulus. The compressibility sum rule relates this instability to a singularity in the static dielectric function $\epsilon(q,0)$ for $q \to 0$. As shown previously,[7] and as is readily seen from (4), the static dielectric function with dynamical-exchange effects indeed diverges in the limit $q \to 0$ at $r_s = 6.0292$. This instability originates from a zero in the denominator $[1 - G(q,0)Q_0(q,0)]$ of $\epsilon(q,0)$ in (1) for $q \to 0$ at $r_s = 6.0292$.

Due to the peak in $G(q,0)$, a zero in the denominator of (1), not only occurs in the long-wavelength limit, but also at finite wavelength. Because $G(kk_F,0)$ is a universal function of k for all densities as shown in Paper I, and $Q_0(kk_F,0)$, considered as a function of k, is proportional to r_s, the critical r_s value for this singularity at finite k is found from

$$1/r_s^{\mathrm{crit}}(k) = G(kk_F,0)[Q_0(kk_F,0)]\big|_{r_s=1}. \qquad (19)$$

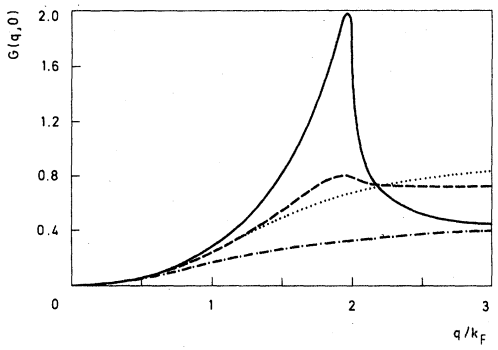

FIG. 1. Local-field correction $G(q,o)$ in the static limit as calculated from the present dynamical-exchange decoupling (——), compared to the approximations of Hubbard (Ref. 2) (-·-·-·), Toigo and Woodruff (Ref. 11) (---), and Vashishta and Singwi (Ref. 22) at $r_s = 3$ (·····).

In Fig. 2, these critical values for r_s are plotted and compared to the critical r_s values, as obtained from the Hubbard approximation[2]

$$G_{\mathrm{Hub}}(q) = \tfrac{1}{2}q^2/(q^2 + k_s^2), \qquad (20)$$

where the screening constant k_s^2 is put equal to $2k_F^2$ in order to satisfy the compressibility sum rule.

Because of this choice of k_s^2, the singularities in $\epsilon(q,0)$ resulting from the Hubbard approximation and from the dynamical-exchange decoupling coincide at $r_s = 6.0292$ in the long-wavelength limit. For increasing wave vector, the critical r_s value increases monotonically in the Hubbard approximation. This is in contrast to the dynamical-exchange-decoupling method, where the rapid increase of $G(q,0)$ to a peak near $q = 2k_F$ results in a decrease of the critical r_s values to a minimum at $r_s \simeq 5$ near $q \simeq 1.85k_F$. With the dynamical-exchange decoupling, the increase in $G(q,0)$ as a function of q overcompensates the decrease in the Lindhard polarizability, so that the product $Q_0(q,0)G(q,0)$ equals 1 at smaller r_s than for $q \to 0$. As will be discussed below, these critical values of r_s are related to an instability, derived by Hamann and Overhauser[3] (hereafter referred to as HO).

Another consequence of the peak in $G(q,0)$ is the occurrence of a zero in the static dielectric function for $r_s \geq 10.6$. One readily obtains from (1) that $\epsilon(q,0)$ is zero if $Q_0(q,0)[G(q,0) - 1] = 1$. Because $Q_0(q,0)$ is positive, and $G(q,0)$ exceeds 1 in the peak near $q = 2k_F$, this equation has been

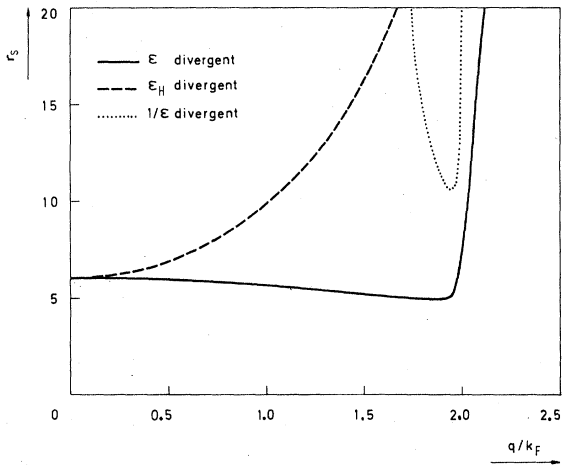

FIG. 2. Critical r_s values as a function of q/k_F for which $\epsilon(q,o)$ with dynamical exchange diverges (——) compared to these critical values from the Hubbard approximation (---). The dotted curve indicates the r_s value for which $\epsilon(q,o)$ has a zero, and thus $1/\epsilon(q,o)$ diverges.

solved for r_s in the region where $G(q,0)>1$. The r_s values for which $\epsilon(q,0)=0$ are also plotted in Fig. 2. A minimum in these critical values of r_s as a function of q is found for $r_s \simeq 10.6$ near $q \simeq 1.94 k_F$. These critical r_s values determine a (q, r_s) region with $1/\epsilon(q,0)$ negative, and thus where the electron gas is unstable relative to the occurrence of charge-density waves, because $1/\epsilon(q,0)$ is the ratio between the total effective potential and the external applied potential. If $\epsilon(q,0)$ is negative, the induced charge density overcompensates the external charge density.

In Fig. 3, $1/\epsilon(q,0)$ is plotted as a function of q for $r_s=3$, 4.92, 5.64, 7.67, and 12.79. These r_s values are chosen for comparison with HO later in this paper. At $r_s=3$ [Fig. 3(a)], no special structure in $1/\epsilon(q,0)$ arises from exchange effects. But at $r_s=4.92$, i.e., just below the minimal critical value of r_s defined by (19), pronounced structure compared to RPA appears for $q<2k_F$ [Fig.

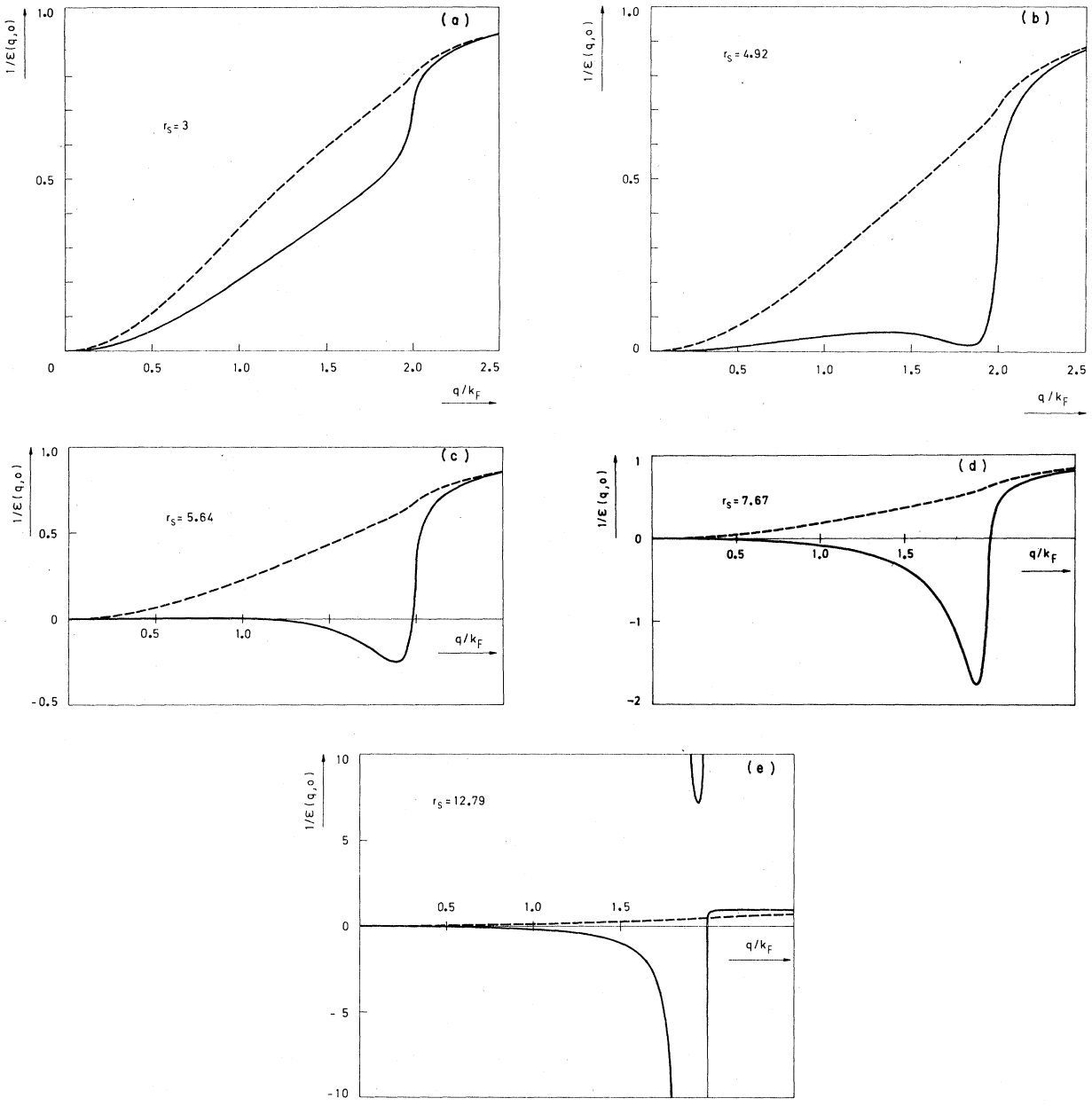

FIG. 3. Inverse static dielectric function with dynamical-exchange decoupling as a function of wave vector (——), and compared to RPA (---) for (a) $r_s=3$, (b) 4.92, (c) 5.64, (d) 7.67, and (e) 12.79.

3(b)]. For $r_s \geq 5$, the dynamical-exchange decoupling, combined with a paramagnetic homogeneous ground state, becomes meaningless, and a region appears where $1/\epsilon(q,0)$ is negative, as shown in Fig. 3(c) for $r_s = 5.64$. With still increasing r_s (>6.0292), the reqion of negative $1/\epsilon(q,0)$ spreads out and includes $q=0$, according to the compressibility sum rule, as shown in Fig. 3(d) for $r_s = 7.67$.

Furthermore, if $1/\epsilon(q,0)$ is negative, it shows a steep structure near $q = 2k_F$. The negative peak increases in magnitude with increasing r_s, and tends to $-\infty$ at $r_s = 10.6$, where $\epsilon(q,0)$ has a zero. For $r_s > 10.6$, a region of positive $1/\epsilon(q,0)$ appears inbetween the two q values satisfying $\epsilon(q,0)=0$, as is shown in Fig. 3(e) for $r_s = 12.79$. In Fig. 4, the corresponding plots for $\epsilon(q,0)$ are given for $r_s = 3$, 4.92, 5.64, 7.67, and 12.79.

An instability, similar to the one obtained here

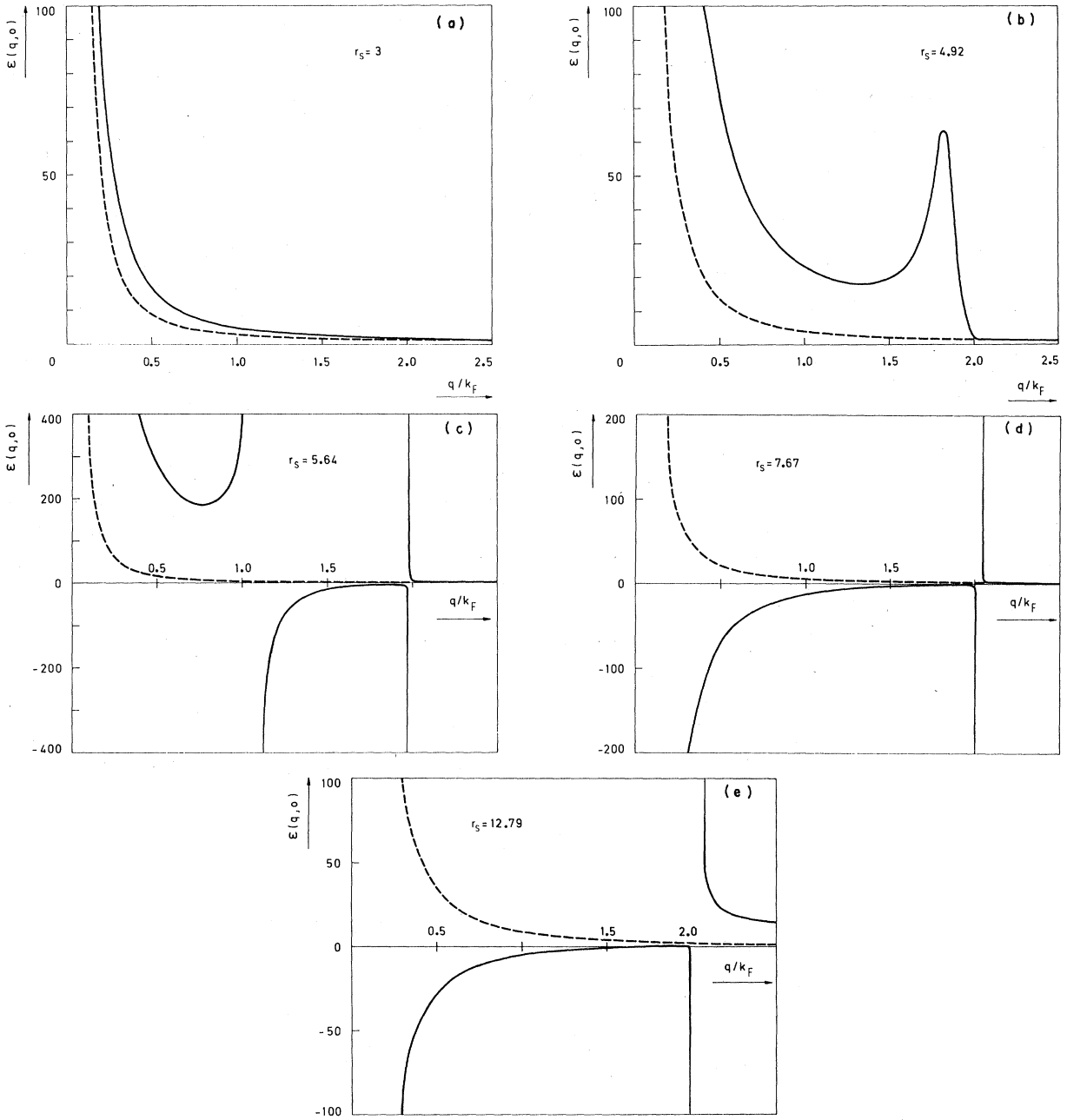

FIG. 4. Static dielectric function with dynamical-exchange decoupling as a function of wave vector (——), and compared to the RPA (---) for (a) $r_s = 3$, (b) 4.92, (c) 5.64, (d) 7.67, and (e) 12.79.

from the dynamical-exchange decoupling, has been derived and discussed by HO.[3] These authors studied the stability of the electron gas in the paramagnetic state, relative to small deformations of the spin magnetization.

In a first approximation, using the Thomas-Fermi screening with a small screening parameter, HO obtained a static dielectric function which behaves very similar to the one we obtain from the dynamical-exchange decoupling. (Figure 2 in HO corresponds to $r_s=4.92$, and Fig. 3 to $r_s=5.64$.) However, at larger r_s (see Fig. 4 in HO, which is at $r_s=7.67$), HO found a supplementary divergence in the dielectric function, arising from the $q\to 0$ limit, whereas with dynamical-exchange decoupling the unstable region has then spread out to include the limit $q\to 0$. For still larger r_s (see Fig. 5 in HO, corresponding to $r_s=12.79$) HO again find the same qualitative picture as is obtained with the dynamical-exchange decoupling. The fact that the HO approach is not completely compatible with the dynamical-exchange decoupling might be due to the use of the Thomas-Fermi screening by Hamann and Overhauser, which seems not well adapted at finite wavelength.

In a second approximation, HO then tried to include some correlation effects by considering the excitations near the Fermi sphere as independent quasiparticles, interacting with an applied test charge which is screened by the electron gas. It is remarkable that this attempt to take correlation into account, stabilizes the paramagnetic state relative to infinitesimal magnetic deformations. However, it is not clear whether the disappearance of the instability with this approximation is due to correlation effects, or to the mathematical approximation of averaging out the momentum dependence in the integrals over the effective interaction.

It should be noted that the static dielectric function discussed here does not provide a reliable description of the instability. Its critical behavior only indicates that, in the critical region, the possibility of spin- or charge-density waves should already have been included in the equilibrium distribution function of the electron gas. In the present paper and in Paper I, a homogeneous equilibrium distribution function was assumed, and the critical behavior of the dielectric function determines the region where the instability has to be built in, but does not describe it. A discussion of the consequences of this instability on the equilibrium properties is given in Ref. 19 and references cited there. Up to now, we did not investigate their effect on the dielectric response properties.

IV. FREQUENCY-DEPENDENT $\epsilon(q,\omega)$ WITH DYNAMICAL-EXCHANGE DECOUPLING

A. Dynamical behavior of $G(q,\omega)$

Our frequency-dependent expression for the local-field correction $G(q,\omega)$ has been evaluated numerically in two independent ways, as described in Paper I.

In order to save computation time, it is worthwhile to remember the theorem that, in the units $q=kk_F$ and $\omega=2\nu E_F/\hbar$, $G(kk_F, 2\nu E_F/\hbar)$ is a universal function of k and ν for all densities. In Paper I, it was shown that

$$G(kk_F, 2\nu E_F/\hbar)=\frac{2\pi^2}{k}f(k,\nu)\int_{-1}^{1}dz\,\mathcal{T}(z,k)\left(\frac{1}{\nu+i\epsilon-\frac{1}{2}k^2-kz}-\frac{1}{\nu+i\epsilon+\frac{1}{2}k^2+kz}\right), \tag{21}$$

where $f(k,\nu)$ and $\mathcal{T}(z,k)$ are given in Eq. (4) and Eq. (36) of Paper I, and where $\mathcal{T}(z,k)$ can be obtained by performing a single integral numerically. It thus follows that tabulating $\mathcal{T}(z,k)$ at given k as a function of z for $-1\leq z\leq 1$ allows one to compute $G(kk_F, 2\nu E_F/\hbar)$ at arbitrary ν by performing a single numerical integral for each ν. Numerical results for ReG and ImG are plotted in Fig. 5 for several values of k. Numerical values are listed in Table I.

For $\nu=0$, $G(kk_F, 2\nu E_F/\hbar)$ tends to the static limit, displayed in Fig. 1 as a function of k. At $|\nu|=|\frac{1}{2}k^2\pm k|$, the real part of the integral in (21) diverges logarithmically, as discussed in Paper I. Because the factor $f(k,\nu)$ contains $1/Q_0^2(kk_F, 2\nu E_F/\hbar)$, this divergent real part contributes to Im$G(kk_F, 2\nu E_F/\hbar)$ at $\nu=|\frac{1}{2}k^2-k|$, where Im$Q_0(kk_F, 2\nu E_F/\hbar)$ differs from zero. Consequently, with dynamical-exchange decoupling, both Re$G(kk_F, 2\nu E_F/\hbar)$ and Im$G(kk_F, 2\nu E_F/\hbar)$ show a logarithmic singularity at $\nu=|\frac{1}{2}k^2-k|$.

On the other hand, at $\nu=\frac{1}{2}k^2+k$, Im$Q_0(kk_F, 2\nu E_F/\hbar)$ equals zero, and thus only the imaginary part of the integral in (21) contributes to Im$G(kk_F, 2\nu E_F/\hbar)$. At the upper boundary of the particle-hole continuum, the divergence only appears in Re$G(kk_F, 2\nu E_F/\hbar)$, while Im$G(kk_F, 2\nu E_F/\hbar)$ remains finite.

For frequencies above the continuum, both Im$Q_0(kk_F, 2\nu E_F/\hbar)$ and the imaginary part of the integral in (21) are zero, and thus Im$G(kk_F, 2\nu E_F/\hbar)$ is zero above the continuity at $\nu=|\frac{1}{2}k^2+k|$.

With further-increasing frequency, $G(kk_F, 2\nu E_F/\hbar)$

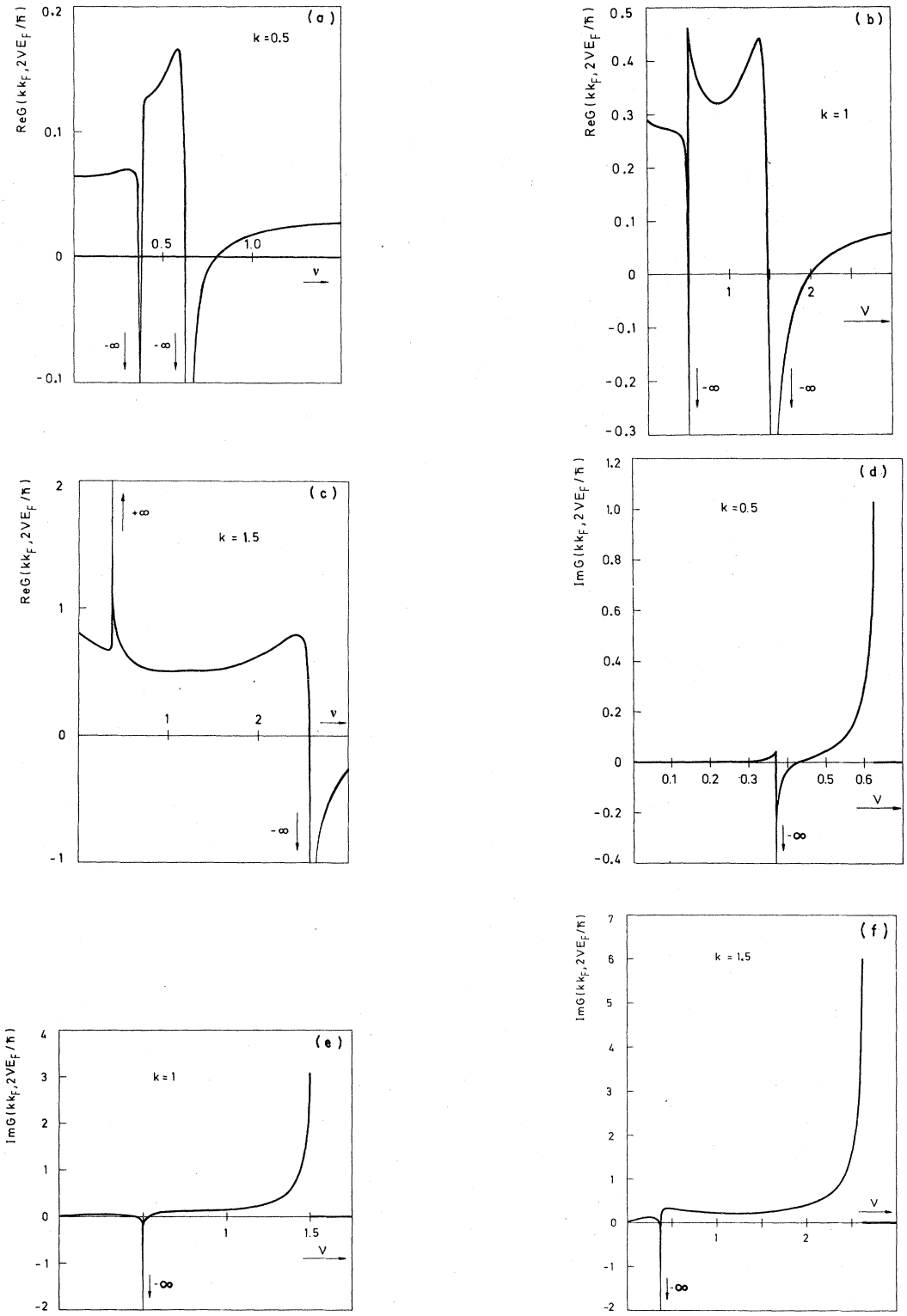

FIG. 5. Real part of $G(kk_F, 2\nu E_F/\hbar)$ with dynamical-exchange decoupling for (a) $k=0.5$, (b) 1.0, and (c) 1.5 and imaginary part of $G(kk_F, 2\nu E_F/\hbar)$, also for (d) $k=0.5$, (e) 1.0, and (f) 1.5, as a function of the reduced frequency ν.

TABLE I. Real and imaginary parts of $G(kk_F, 2\nu E_F/\hbar)$ for several values of k and ν.

$k=0.2$			$k=0.4$			$k=0.6$			$k=0.8$			$k=1.0$		
ν	ReG	ImG	ν	ReG	ImG	ν	ReG	ImG	ν	ReG	ImG	ν	ReG	ImG
0	0.0101	0	0	0.0405	0	0	0.0943	0	0	0.1761	0	0	0.2898	0
0.0400	0.0103	-1.28×10^{-4}	0.0800	0.0412	5.74×10^{-4}	0.0800	0.0940	2.26×10^{-3}	0.0800	0.1724	5.63×10^{-3}	0.0800	0.2830	0.0126
0.0800	0.0107	-2.06×10^{-4}	0.1600	0.0435	1.57×10^{-3}	0.1600	0.0939	3.12×10^{-3}	0.1600	0.1716	8.62×10^{-3}	0.1600	0.2780	0.0191
0.1200	0.0117	-0.92×10^{-4}	0.2400	0.0463	2.05×10^{-3}	0.2400	0.0952	4.71×10^{-3}	0.2400	0.1686	0.0109	0.2400	0.2735	0.0209
0.1500	0.0135	1.25×10^{-3}	0.3000	0.0452	0.0140	0.3200	0.0965	6.52×10^{-3}	0.3200	0.1721	0.0125	0.3200	0.2679	0.0229
0.1726	0.0176	7.04×10^{-3}	0.3100	0.0372	0.0232	0.3900	0.0854	0.0147	0.4000	0.1623	0.0133	0.4000	0.2587	0.0212
0.1782	0.0135	0.0253	0.3151	0.0195	0.0358	0.4126	0.0292	0.0256	0.4400	0.1537	0.0161	0.4400	0.2558	0.0157
0.1796	−0.0133	0.0514	0.3188	−0.0431	0.0549	0.4182	−0.0727	0.0072	0.4600	0.1167	0.0069	0.4701	0.2160	−0.0016
0.1800	$-\infty$	$+\infty$	0.3195	−0.0824	0.0615	0.4196	−0.2035	−0.0351	0.4700	0.0715	−0.0080	0.4851	0.1751	−0.0341
0.1803	−0.1184	0.0393	0.3199	−0.1937	0.0745	0.4199	−0.2933	−0.0676	0.4776	−0.0431	−0.0817	0.4926	0.1244	−0.0901
0.1812	−0.0235	−0.0226	0.3200	$-\infty$	$+\infty$	0.4200	$-\infty$	$-\infty$	0.4795	−0.1722	−0.1922	0.4982	0.0274	−0.2454
0.1850	0.0200	−0.0175	0.3205	−0.2527	−0.0922	0.4201	−2.701	−1.278	0.4799	−0.3369	−0.3455	0.4999	−0.1450	−0.5917
0.2000	0.0404	0.0135	0.3212	−0.0935	−0.1010	0.4208	−0.2647	−0.3399	0.4800	$-\infty$	$-\infty$	0.5000	$-\infty$	$-\infty$
0.2100	0.0466	0.0419	0.3249	0.0397	−0.0799	0.4236	0.0707	−0.1882	0.4801	−5.503	−5.788	0.5001	−2.941	−7.622
0.2150	0.0453	0.0795	0.3300	0.0676	−0.0509	0.4274	0.1325	−0.1345	0.4812	−0.0748	−0.5834	0.5008	0.0303	−1.252
0.2175	0.0255	0.1323	0.3400	0.0815	−0.0289	0.4349	0.1579	−0.0791	0.4849	0.2320	−0.2515	0.5074	0.4618	−0.2194
0.2194	−0.0797	0.2102	0.3600	0.0947	−0.0027	0.4499	0.1671	−0.0391	0.4899	0.2796	−0.1567	0.5149	0.4628	−0.0987
0.2199	−0.2194	0.2444	0.4000	0.1050	0.0349	0.4800	0.1701	−0.0013	0.5000	0.2845	−0.0807	0.5299	0.4325	−0.0229
0.2200	$-\infty$	0.2575	0.4400	0.1205	0.0990	0.5200	0.1698	0.0260	0.5200	0.2847	−0.0217	0.5600	0.4005	0.0440
0.2201	−0.9775	0	0.4600	0.1171	0.1901	0.5600	0.1724	0.0450	0.5600	0.2664	0.0192	0.6000	0.3688	0.0744
0.2274	−0.0299	0	0.4701	0.0865	0.2975	0.6000	0.1786	0.0679	0.6400	0.2516	0.0575	0.8000	0.3255	0.1182
0.2500	−0.00680	0	0.4776	−0.1385	0.5469	0.6400	0.1884	0.0973	0.7200	0.2473	0.0828	1.0000	0.3309	0.1529
0.2800	−0.00234	0	0.4788	−0.3125	0.6236	0.6800	0.2046	0.1452	0.8000	0.2553	0.1095	1.2000	0.3778	0.2444
0.3200	0.00112	0	0.4799	−0.9768	0.7185	0.7200	0.2149	0.2405	0.8800	0.2705	0.1494	1.4000	0.4409	0.6580
0.3600	0.00210	0	0.4800	$-\infty$	0.7295	0.7500	0.1953	0.4171	0.9600	0.2984	0.2275	1.4400	0.3900	0.9532
0.4000	0.00264	0	0.4805	−1.3070	0	0.7651	0.1114	0.6216	1.0400	0.3222	0.4274	1.4701	0.1834	1.400
0.8000	0.00394	0	0.4849	−0.2457	0	0.7726	−0.0624	0.8647	1.1000	0.1205	1.031	1.4851	−0.1769	1.917
1.2000	0.00413	0	0.4900	−0.1507	0	0.7782	−0.673	1.191	1.1101	−1.1679	1.402	1.4926	−0.7821	2.365
1.6000	0.00420	0	0.5000	−0.0868	0	0.7799	−1.916	1.349	1.1176	−1.123	1.889	1.4964	−1.503	2.665
2.0000	0.00423	0	0.6000	−0.0040	0	0.7800	$-\infty$	1.358	1.1188	−1.659	2.008	1.4992	−3.058	2.961
3.0000	0.00426	0	0.8000	0.0121	0	0.7801	−15.25	0	1.1195	−2.209	2.078	1.4999	−5.041	3.061
4.0000	0.00427	0	1.2000	0.0178	0	0.7874	−0.5095	0	1.1199	−3.591	2.140	1.5000	$-\infty$	3.083
			1.6000	0.0194	0	0.7949	−0.3229	0	1.1200	$-\infty$	2.154	1.5018	−0.6206	0
			2.0000	0.0200	0	0.8100	−0.1931	0	1.1202	−16.30	0	1.5074	−0.5802	0
			3.0000	0.0207	0	0.8400	−0.1011	0	1.1224	−2.144	0	1.5149	−0.5519	0
			4.0000	0.0209	0	0.9200	−0.0276	0	1.1299	−0.8521	0	1.5299	−0.4908	0
						1.0000	−0.0024	0	1.1400	−0.5531	0	1.5600	−0.3745	0
						1.2000	0.0214	0	1.1600	−0.3404	0	1.6000	−0.2698	0
						1.6000	0.0351	0	1.2000	−0.1865	0	1.6800	−0.1501	0
						2.0000	0.0398	0	1.2800	−0.0744	0	1.7600	−0.0859	0
						3.0000	0.0436	0	1.3600	−0.0298	0	1.8400	−0.0465	0

TABLE I. *(Continued.)*

$k=0.2$			$k=0.4$			$k=0.6$			$k=0.8$			$k=1.0$		
ν	ReG	ImG	ν	ReG	ImG	ν	ReG	ImG	ν	ReG	ImG	ν	ReG	ImG
						4.0000	0.0449	0	1.4800	0.0043	0	1.9200	−0.0196	0
									1.5600	0.0177	0	2.0000	−0.0001	0
									1.6400	0.0274	0	2.1200	0.0208	0
									1.7600	0.0376	0	2.2400	0.0356	0
									1.8800	0.0447	0	2.3600	0.0465	0
									2.0000	0.0499	0	2.4800	0.0550	0
									3.0000	0.0669	0	2.6000	0.0617	0
									4.0000	0.0714	0	2.8000	0.0702	0
												3.0000	0.0765	0
												3.4000	0.0851	0
												3.8000	0.0905	0
												4.0000	0.0925	0
	$k=1.2$			$k=1.4$			$k=1.6$			$k=1.8$			$k=2.0$	
ν	ReG	ImG	ν	ReG	ImG	ν	ReG	ImG	ν	ReG	ImG	ν	ReG	ImG
0	0.4492	0	0	0.6733	0	0	0.9924	0	0	1.462	0	0	1.531	0
0.0800	1.4336	0.0261	0.0800	0.6418	0.0520	0.0800	0.9292	0.1085	0.0800	1.312	0.2432	0.0800	1.255	0.2796
0.1600	0.4221	0.0361	0.1600	0.6164	0.0716	0.1600	0.8780	0.1494	0.1200	1.246	0.2932	0.1600	1.108	0.3047
0.2400	0.4123	0.0425	0.2400	0.5972	0.0833	0.2400	0.8371	0.1553	0.1501	1.207	0.2909	0.2400	1.023	0.3022
0.3200	0.3996	0.0446	0.3200	0.5719	0.0836	0.3000	0.8223	0.0720	0.1651	1.225	0.2551	0.3200	0.9690	0.2984
0.4000	0.3884	0.0348	0.3600	0.5683	0.0636	0.3101	0.8537	−0.0147	0.1764	1.347	0.1601	0.4000	0.9290	0.2939
0.4400	0.3602	0.0094	0.3901	0.5431	0.0204	0.3151	0.9059	−0.1085	0.1782	1.441	0.1026	0.4800	0.8957	0.2920
0.4600	0.3276	−0.0373	0.4051	0.5289	−0.0595	0.3188	1.049	−0.3162	0.1799	1.794	−0.0971	0.5600	0.8586	0.2812
0.4701	0.2942	−0.1151	0.4126	0.5351	−0.1613	0.3199	1.342	−0.7038	0.1800	$+\infty$	$-\infty$	0.6400	0.8424	0.2855
0.4776	0.2512	−0.3157	0.4182	0.5808	−0.3928	0.3200	$+\infty$	$-\infty$	0.1801	15.28	−6.984	0.7200	0.8236	0.2827
0.4788	0.2359	−0.4362	0.4199	0.7089	−0.8619	0.3202	6.256	−6.157	0.1836	1.723	0.4665	0.8000	0.8078	0.2803
0.4799	0.1953	−0.8765	0.4200	$+\infty$	$-\infty$	0.3224	1.655	−0.2062	0.1949	1.249	0.6263	1.0000	0.7806	0.2789
0.4800	$-\infty$	$-\infty$	0.4201	5.004	−13.68	0.3299	1.195	0.3050	0.2099	1.082	0.5892	1.2000	0.7595	0.2758
0.4802	0.3278	−5.730	0.4218	1.256	−0.7776	0.3400	1.039	0.3935	0.2400	0.9919	0.5064	1.4000	0.7513	0.2811
0.4812	0.6769	−1.204	0.4274	0.9986	−0.0252	0.3600	0.8919	0.4018	0.2800	0.9200	0.4797	1.6000	0.7490	0.2880
0.4849	0.7231	−0.2895	0.4349	0.9009	0.1268	0.4000	0.7986	0.3745	0.3200	0.8635	0.4501	1.8000	0.7446	0.2968
0.4899	0.7025	−0.1055	0.4499	0.7893	0.2021	0.6000	0.6284	0.3133	0.4000	0.8018	0.3991	2.0000	0.7574	0.3067
0.5000	0.6480	0.0175	0.4800	0.6969	0.2434	0.8000	0.5745	0.2797	0.6000	0.7129	0.3368	2.2000	0.7748	0.3308
0.5200	0.5851	0.0810	0.5200	0.6252	0.2348	1.0000	0.5484	0.2594	0.8000	0.6701	0.2978	2.4000	0.7968	0.3635
0.5600	0.5153	0.1328	0.6000	0.5642	0.2421	1.2000	0.5524	0.2503	1.0000	0.6542	0.2839	2.6000	0.8258	0.4031
0.6400	0.4606	0.1526	0.8000	0.4952	0.2263	1.4000	0.5546	0.2543	1.2000	0.6399	0.2735	2.8000	0.8704	0.4620
0.7200	0.4279	0.1620	1.0000	0.4716	0.2176	1.6000	0.5676	0.2703	1.4000	0.6405	0.2760	3.0000	0.9258	0.5515
0.8000	0.4128	0.1638	1.2000	0.4729	0.2184	1.8000	0.5919	0.2992	1.6000	0.6474	0.2787	3.2000	0.9928	0.6868
1.0000	0.3977	0.1747	1.4000	0.4855	0.2368	2.0000	0.6288	0.3496	1.8000	0.6557	0.2993	3.4000	1.093	0.9086
1.2000	0.4101	0.1965	1.6000	0.5144	0.2737	2.2000	0.6833	0.4401	2.0000	0.6778	0.3207	3.6000	1.199	1.328
1.4000	0.4429	0.2510	1.8000	0.5636	0.3560	2.4000	0.7632	0.6056	2.2000	0.7038	0.3539	3.7200	1.252	1.816

TABLE I. *(Continued.)*

$k=1.2$			$k=1.4$			$k=1.6$			$k=1.8$			$k=2.0$		
ν	ReG	ImG	ν	ReG	ImG	ν	ReG	ImG	ν	ReG	ImG	ν	ReG	ImG
1.6000	0.5096	0.3933	2.0000	0.6400	0.5233	2.6000	0.8609	0.9958	2.4000	0.7511	0.4133	3.8000	1.218	2.366
1.8000	0.5715	0.9264	2.2000	0.7219	1.011	2.6800	0.8804	1.322	2.6000	0.8072	0.5009	3.8800	0.9764	3.342
1.8400	0.5164	1.239	2.2800	0.6541	1.568	2.7200	0.8641	1.575	2.8000	0.8799	0.6554	3.9600	−0.4619	5.682
1.8800	0.2488	1.839	2.3200	0.4313	2.144	2.7600	0.8053	1.931	3.0000	0.9832	0.9519	3.9901	−4.354	8.217
1.9000	−0.2041	2.512	2.3501	−0.0713	2.956	2.8000	0.6088	2.503	3.2000	1.055	1.674	3.9988	−11.39	9.472
1.9101	−0.9850	3.129	2.3651	−0.9486	3.811	2.8400	0.0254	3.486	3.2400	1.035	1.953	3.9999	−19.97	9.702
1.9151	−1.934	3.550	2.3764	−3.416	4.828	2.8600	−0.9618	4.573	3.2800	0.9600	2.337	4.0000	$-\infty$	9.729
1.9188	−3.954	3.965	2.3792	−6.103	5.199	2.8701	−2.379	5.410	3.3200	0.7951	2.902			
1.9199	−7.652	4.131	2.3799	−9.514	5.320	2.8776	−5.582	6.272	3.3600	0.3039	3.783			
1.9200	$-\infty$	4.134	2.3800	$-\infty$	5.347	2.8799	−13.12	6.657	3.3901	−0.6535	5.080			
1.9205	−0.7334	0	2.3808	−0.7939	0	2.8800	$-\infty$	6.674	3.4051	−2.226	6.249			
1.9399	−0.6591	0	2.3949	−0.7859	0	2.8823	−0.9180	0	3.4126	−4.104	7.037			
1.9600	−0.5969	0	2.4400	−0.6805	0	2.8999	−0.8485	0	3.4199	−15.320	8.107			
2.0000	−0.4643	0	2.5200	−0.4804	0	2.9199	−0.8211	0	3.4200	$-\infty$	8.132			
2.2000	−0.1596	0	2.6000	−0.3449	0	2.9600	−0.7474	0	3.4274	−0.9416	0			
2.4000	−0.0526	0	2.8000	−0.1602	0	3.0000	−0.6701	0	3.4499	−0.9357	0			
2.6000	0.0008	0	3.0000	−0.0694	0	3.2000	−0.3532	0	3.4800	−0.9003	0			
2.8000	0.0329	0	3.2000	−0.0151	0	3.4000	−0.1987	0	3.5200	−0.7723	0			
3.0000	0.0543	0	3.4000	0.0209	0	3.6000	−0.1069	0	3.6000	−0.6688	0			
3.2000	0.0694	0	3.6000	0.0461	0	3.8000	−0.0484	0	3.8000	−0.4172	0			
3.4000	0.0806	0	3.8000	0.0652	0	4.0000	−0.0061	0	4.0000	−0.2719	0			
3.6000	0.0893	0	4.0000	0.0797	0									
3.8000	0.0962	0												
4.0000	0.1017	0												

approaches the high-frequency limit, calculated in Appendix A of Paper I.

B. Dynamical behavior of $\epsilon(q,\omega)$ and plasmon dispersion

Because $G(kk_F, 2\nu E_F/\hbar)$ is a universal function of k and ν for all densities, the density dependence in $\epsilon(kk_F, 2\nu E_F/\hbar)$ as a function of k and ν only enters via the Lindhard polarizability $Q_0(kk_F, 2\nu E_F/\hbar)$, which, as a function of k and ν, only depends on the density by the proportionality factor r_s. Therefore, the numerical evaluation of $\epsilon(kk_F, 2\nu E_F/\hbar)$ at an arbitrary density is rather straightforward, given the values of $G(kk_F, 2\nu E_F/\hbar)$ in Table I. Because of the logarithmic singularity, it is rather important that this table contains many points near $\nu = \left|\frac{1}{2}k^2 \pm k\right|$.

For relatively small r_s, the dielectric function with dynamical exchange included is not much different from RPA, except for the exchange effects near $\nu = \left|\frac{1}{2}k^2 \pm k\right|$. But with increasing r_s, overall exchange effects appear in the numerical values, as is manifest from the plots of $\mathrm{Re}\epsilon(q,\omega)$, presented in Paper I for $r_s = 2$ and in Ref. 20 for $r_s = 3$.

The singularity in $\mathrm{Re}\epsilon(q,\omega)$ near $\omega = \hbar(\frac{1}{2}q^2 + qk_F)/m$ is related to the logarithmic singularity in $G(q,\omega)$, which is an artifact due to the cutoff in the Fermi function. Although a singularity also occurs in $G(q,\omega)$ at $\omega = \hbar\left|\frac{1}{2}q^2 - qk_F\right|/m$, it does not produce a pole in $\mathrm{Re}\epsilon(q,\omega)$, but only a strongly peaked structure, because $Q_0(q,\omega)$ has an imaginary part in this region.

In Paper I and in Ref. 20, $\mathrm{Im}[1/\epsilon(q,\omega)]$ has been shown for $r_s = 2$ and $r_s = 3$ for several values of q. The logarithmic singularity in $G(q,\omega)$ at $\omega = \hbar\left|\frac{1}{2}q^2 - qk_F\right|/m$ induces a zero in $\mathrm{Im}[1/\epsilon(q,\omega)]$. However, the width of this dip is so small that one hardly expects it to be important for comparison with experiment.

Another consequence of the logarithmic singularity is found in the behavior of the plasmon dispersion. As already mentioned in Ref. 20, the plasmon, defined by $\mathrm{Re}\epsilon(q,\omega) = 0$ outside the continuum, does not penetrate into the particle-hole continuum, but approaches it asymptotically. However, the physically relevant property is the frequency at the maximum in the structure factor. The oscillator strength of the plasmon is proportional to $[d\epsilon(q,\omega)/d\omega]^{-1}$ at the plasmon frequency. $\mathrm{Re}\epsilon(q,\omega)$ is a very steep function of ω near its zero when this zero approaches the continuum. Consequently, the derivative with respect to frequency at the plasmon frequency becomes very large, and thus the plasmon oscillator strength decreases rapidly with increasing wave vector. The maximum in the structure factor is then no longer defined by the plasmon peak position, but by the maximum of the inverse dielectric function inside the continuum.

At finite wave vector, the frequencies of the maxima in the structure factor with dynamical-exchange decoupling are appreciably lowered compared to RPA.[21] This is a trend which is confirmed by recent electron scattering experiments in Al.[4] In Fig. 6, the maxima in $\mathrm{Im}[1/\epsilon(q,\omega)]$ with dynamical-exchange decoupling are shown for $r_s = 2$, and compared to RPA and to the experimental data for Al ($r_s = 2.07$). The position of the plasmon peak in both the exchange and the RPA treatments are also indicated. Keeping in mind that the oscillator strength of the plasmon peak with dynamical-exchange decoupling disappears when it approaches the continuum and is taken over by the maximum in $\mathrm{Im}[1/\epsilon(q,\omega)]$, Fig. 6 clearly shows that, at finite q, the exchange effects considerably

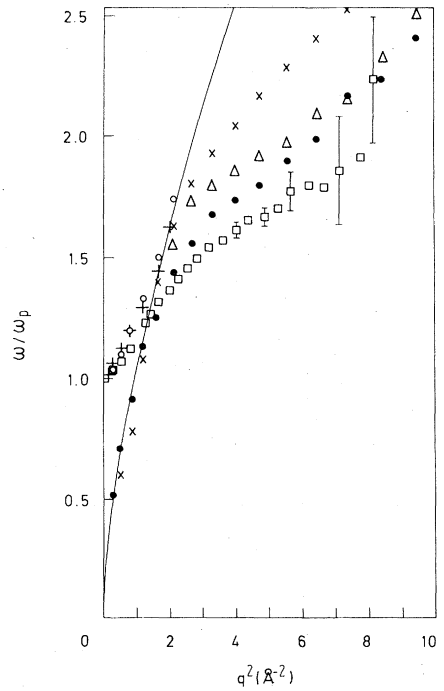

FIG. 6. Plasmon frequency as defined by $\mathrm{Re}\epsilon(q,\omega) = 0$ and peak position of the dynamical structure factor $S(q,\omega)$ versus the square of the wave vector at $r_s = 2$. (See also Ref. 21.) The RPA plasmon is indicated by (○), and the plasmon including dynamical-exchange effects by (+). When the plasmon including exchange approaches the particle-hole continuum (thin line), its oscillator strength is taken over by the maxima of $S(q,\omega)$ (●), which are at substantially lower frequencies than the RPA maxima (×). The experimental data (□) for Al ($r_s = 2.07$) are taken from P. E. Batson, C. H. Chen, and J. Silcox (Ref. 4). The triangles (△) indicate the maxima of $S(q,\omega)$ as obtained from the approximation of P. Vashishta and K. S. Singwi (Ref. 22).

improve the agreement with experiment, compared to RPA.

C. Remark on spin-density waves

In the derivation of $G(q,\omega)$ via the dynamical-exchange decoupling in the equation of motion for the Wigner distribution function, it has been assumed, in line with RPA, that the ground-state distribution of the electron gas is homogeneous in space. This does not seem unreasonable, because it is generally accepted that the transition to a Wigner lattice occurs at densities far below the metallic range.[23]

Furthermore, it was assumed that the ground state is paramagnetic. This assumption is inspired by the fact that the HF ground state in the ferromagnetic state has only lower energy than the paramagnetic HF ground state for $r_s \geq 5.45$. Moreover, the inclusion of correlation presumably shifts the transition into the ferromagnetic state to $r_s \geq 6.03$.[24] However, spin-density waves lower the ground-state energy of the electron gas in the HF approximation.[25] Therefore, it is indicated to examine whether the dielectric function including dynamical-exchange effects, reflects an instability relative to deformations of the paramagnetic state.

Following the derivation of the dielectric function with dynamical-exchange decoupling, as given in detail in Ref. 7, the variational procedure of Ref. 7 can easily be applied for each spin state separately, by introducing a spin-dependent function $\gamma^{\sigma}_{\vec{q}\omega}(\vec{p})$ in Eq. (26) of Ref. 7:

$$\tilde{f}_{\sigma}(\vec{p},\vec{q},\omega)=\tilde{f}^{L}_{\sigma}(\vec{p},\vec{q},\omega)\,\gamma^{\sigma}_{\vec{q}\omega}(\vec{p}). \tag{22}$$

Again determining a momentum-independent function $\gamma^{\sigma}_{\vec{q}\omega}$ by the variational principle, one then obtains, along the lines described in Ref. 7,

$$\gamma^{\sigma}_{\vec{q}\omega}=-\frac{\frac{1}{2}(e\varphi_{\vec{q}\omega}+U_{\vec{q}\omega})Q_0(q,\omega)-(4\pi e^2/q^2)n^{\sigma}_{\vec{q}\omega}}{\frac{1}{2}e\varphi_{\vec{q}\omega}Q_0^2(q,\omega)G(q,\omega)/[1+Q_0(q,\omega)]}, \tag{23}$$

which replaces Eq. (30) of Ref. 7. Subsequently calculating the density for both spins from (22), one obtains two coupled equations:

$$n^{\uparrow}_{\vec{q}\omega}[Q_0(q,\omega)G(q,\omega)-1-\tfrac{1}{2}Q_0(q,\omega)]-\tfrac{1}{2}n^{\downarrow}_{\vec{q}\omega}Q_0(q,\omega)$$
$$=\tfrac{1}{2}e\varphi_{\vec{q}\omega}\frac{q^2}{4\pi e^2}Q_0(q,\omega), \tag{24}$$

and the same equation with $n^{\uparrow}_{\vec{q}\omega}$ and $n^{\downarrow}_{\vec{q}\omega}$ interchanged. From these equations, one readily obtains $n_{\vec{q}\omega}\equiv n^{\uparrow}_{\vec{q}\omega}+n^{\downarrow}_{\vec{q}\omega}$. However, both equations are only linearly independent, with $n^{\uparrow}_{\vec{q}\omega}=n^{\downarrow}_{\vec{q}\omega}$, if $1-G(q,\omega)Q_0(q,\omega)$ differs from zero. If, however, the condition

$$1-G(q,\omega)Q_0(q,\omega)=0 \tag{25}$$

is fulfilled, the relative contribution of spins up and spins down to the density remains undetermined. The condition (25) implies a singularity in the dielectric function.

For the static limit, the instability (25) has already been discussed in Sec. III. In the dynamical case $\omega\neq 0$, however, $G(q,\omega)$ has a logarithmic singularity at $\omega=\hbar(\frac{1}{2}q^2+qk_F)/m$ for all densities, which is responsible for the fact that $\epsilon(q,\omega)$ with dynamical-exchange decoupling has a pole slightly above the particle-hole continuum for all densities. The occurrence of this pole is expressed by condition (25), which is the dynamical extension of the static instability discussed by HO.[3]

The occurrence of this pole in $\epsilon(q,\omega)$ does not necessarily imply the existence of spin-density waves from dynamical-exchange effects in the homogeneous electron gas. It only means that the stability of the paramagnetic state has to be reexamined with respect to small density deformations. This possibility of an instability already should be included in the initial state. Up until now, the consequences on the dynamical-exchange decoupling have not been studied.

Furthermore, the question arises whether this possibility for the occurrence of spin-density waves is a property of the electron-gas model, or is a consequence of the neglect of correlations.

Although in the static limit these correlation effects have, to some extent, been studied in Ref. 3, the existence of a pole in the *dynamical* dielectric function, and its relation to the possibility of spin-density waves, has not been pointed out before. This pole is due to dynamical-exchange effects starting from a paramagnetic ground state, but the influence of dynamical-correlation effects, and of deviations from the paramagnetic initial state, remains to be studied.

V. CONCLUSION

In this study (Papers I and II), the bare exchange effects in the electron gas have been included in the equation of motion for the Wigner distribution function $f_{\sigma}(\vec{p},\vec{R},t)$ using the dynamical-exchange decoupling. The variational solution for $f_{\sigma}(\vec{p},\vec{R},t)$ rigorously satisfies the equation of motion for the induced charge and current density including exchange. Therefore, the dynamical-exchange effects in the dielectric function are adequately described by the resulting frequency-dependent expression for the local-field correction $G(q,\omega)$, as is confirmed by the analytical evaluation of several limits in the present paper.

The dynamical-exchange-decoupling method is the only known method leading to $g(0)=\frac{1}{2}$, both from the static limit of $G(q,\omega)$ and from the frequency de-

pendence of $\epsilon(q,\omega)$.

In the static limit, it is also shown that the compressibility, obtained from the dielectric function derived here, is consistent with the HF results.

Furthermore, also if the third-frequency moment is used, the high-frequency limit of $G(q,\omega)$ leads to $g(0)=\frac{1}{2}$. Moreover, this high-frequency limit is shown to be consistent with the well-known HF ground-state energy.

This internal consistency of the dynamical-exchange treatment, which we proved from several analytical limits, seems consistent with the conservation of frequency moments to infinite order, in the HF approximation.[8]

The numerical evaluation of $G(q,\omega)$ in the static limit reveals a peak in $G(q,0)$ near $q=2k_F$, confirming Sham's conjecture.[9] This peak has important effects on the behavior of the static dielectric function. Apart from the instability of the electron gas in the long-wavelength limit at $r_s=6.0292$ (which one expects as a consequence of the compressibility sum rule), the structure in $G(q,0)$ yields a divergence in $\epsilon(q,0)$ at *finite wave vector* for $r_s \geq 5$, and thus induces an instability at low densities. This instability is of the same nature as the one due to the spin susceptibility, discussed in another context in Ref. 3. Moreover, a supplementary instability shows up at still lower densities ($r_s \geq 10.6$), corresponding to induced deformations in the charge density. The effect of including correlation on these instabilities remains to be examined.

In the present work, the frequency dependence of the local-field correction was also studied numerically, and several plots of $\mathrm{Re}G(q,\omega)$ and $\mathrm{Im}G(q,\omega)$ are presented. This frequency dependence has pronounced effects on the dielectric function, which is also shown for several densities. One of these effects is that, compared to RPA, the inclusion of dynamical-exchange effects lowers the frequencies of the maxima in the dynamical structure factor, yielding relatively good overall agreement with experimental data in Al.

A very striking feature of the dynamical-exchange decoupling in the dielectric function is a pole in $\epsilon(q,\omega)$ outside the particle-hole continuum. This pole is attributed to spin-density waves in the electron gas, as predicted from static considerations by Overhauser.[25] Also, in this respect, the correlation effects should be studied, as they might influence this critical behavior substantially.

Note added in proof. The present authors already reported plots of $\mathrm{Re}G(k,\omega)$ as a function of frequency in Bull. Am. Phys. Soc. 22, 438 (1977).

ACKNOWLEDGMENT

This work was partially supported by a research grant of the Sponsored Research Committee of Control Data Corporation, Minneapolis, Minn.

APPENDIX: STATIC STRUCTURE FACTOR FOR $q \to \infty$

In Sec. II, the consistency of the high-frequency limit and the static limit of the frequency-dependent local-field correction has been established by using the static structure factor $S(q)$ in terms of the dielectric function $\epsilon(q,\omega)$:

$$S(q)=-\frac{q^2}{4\pi e^2}\frac{\hbar}{n\pi}\int_0^\infty d\omega\,\mathrm{Im}\frac{1}{\epsilon(q,\omega)}. \tag{A1}$$

$S(q)$ was needed in the limit of large q, $\epsilon(q,\omega)$ is given by (1), and thus the inverse dielectric function is

$$\frac{1}{\epsilon(q,\omega)}=1-\frac{Q_0(q,\omega)}{1+Q_0(q,\omega)-G(q,\omega)Q_0(q,\omega)}. \tag{A2}$$

In the units $q=kk_F$ and $\hbar\omega=2\nu E_F$, (A1) can be rewritten

$$S(kk_F)=-\tfrac{3}{4}a_0k_Fk^2\int_0^\infty d\nu\,\mathrm{Im}\frac{1}{\epsilon(kk_F,2\nu E_F/\hbar)}. \tag{A3}$$

In these units, it has been shown in Paper I that

$$Q_0(kk_F,2\nu E_F/\hbar)=\frac{1}{\pi^2a_0k_F}\int d^3r\,\frac{\mathfrak{N}(\vec{r}+\frac{1}{2}\vec{k})-\mathfrak{N}(\vec{r}-\frac{1}{2}\vec{k})}{\nu_+-\vec{r}\cdot\vec{k}}, \tag{A4}$$

$$G(kk_F,2\nu E_F/\hbar)=f(k,\nu)\int d^3r\int d^3r'\,\frac{1}{|\vec{r}-\vec{r}'|^2}\,\frac{1}{\nu_+-\vec{r}\cdot\vec{k}}\left(\frac{1}{\nu_+-\vec{r}'\cdot\vec{k}}-\frac{1}{\nu_+-\vec{r}\cdot\vec{k}}\right)$$
$$\times[\mathfrak{N}(\vec{r}+\vec{k}/2)-\mathfrak{N}(\vec{r}-\vec{k}/2)][\mathfrak{N}(\vec{r}'+\vec{k}/2)-\mathfrak{N}(\vec{r}'-\vec{k}/2)], \tag{A5}$$

with $\nu_+=\nu+i0^+$ and with

$$f(k,\nu)=\frac{1}{\pi^4a_0^2k^2k_F^2}\,\frac{1}{Q_0^2(kk_F,2\nu E_F/\hbar)}. \tag{A6}$$

$\mathfrak{N}(\vec{r})$ is the Fermi function, normalized to 1 if $|\vec{r}|\leq 1$, and zero elsewhere. From (A4) it follows that

$$\mathrm{Im}\int_0^\infty d\nu Q_0(kk_F, 2\nu E_F/\hbar) \underset{k>2}{=} \frac{4}{3}\frac{1}{a_0 k_F}\frac{1}{k^2}. \tag{A7}$$

Furthermore, by using the identity

$$\frac{1}{\nu_+ - \vec{r}\cdot\vec{k}}\,\frac{1}{\nu_+ - \vec{r}'\cdot\vec{k}} = \left(\frac{1}{\nu_+ - \vec{r}\cdot\vec{k}} - \frac{1}{\nu_+ - \vec{r}'\cdot\vec{k}}\right)\frac{1}{\vec{k}\cdot(\vec{r}-\vec{r}')}, \tag{A8}$$

and after performing some elementary translations in the integration variables, Q_0^2 can be written

$$Q_0^2(kk_F, 2\nu E_F/\hbar) = \frac{2}{\pi^4 a_0^2 k_F^2 k^4}\int d^3r \int d^3r' \mathfrak{N}(\vec{r})\mathfrak{N}(\vec{r}')\left[\frac{1}{\nu_+ + \frac{1}{2}k^2 - \vec{r}\cdot\vec{k}}\left(\frac{1}{\vec{k}\cdot(\vec{r}-\vec{r}')} - \frac{1}{\vec{k}\cdot(\vec{r}-\vec{r}'-\vec{k})}\right)\right.$$
$$\left. + \frac{1}{\nu_+ - \frac{1}{2}k^2 - \vec{r}\cdot\vec{k}}\left(\frac{1}{\vec{k}\cdot(\vec{r}-\vec{r}')} - \frac{1}{\vec{k}\cdot(\vec{r}-\vec{r}'+\vec{k})}\right)\right]. \tag{A9}$$

Expressing the integral over $\vec{r}$ in cylindrical coordinates, with the z axis along $\vec{k}$, (A9) becomes

$$Q_0^2(kk_F, 2\nu E_F/\hbar) = -\frac{2}{\pi^4 a_0^2 k_F^2 k^5}\int_{-1}^{1} dz\left(\frac{L(z,-k)-L(z,0)}{\nu_+ + k^2/2 - zk} + \frac{L(z,k)-L(z,0)}{\nu_+ - k^2/2 - zk}\right), \tag{A10}$$

where

$$L(z,k) = \int_0^{(1-z^2)^{1/2}} \rho\, d\rho \int_0^{2\pi} d\varphi \int d^3r' \mathfrak{N}(\vec{r}')\frac{1}{z - z' + k}. \tag{A11}$$

From (A11), $L(z,k)$ has the symmetry property

$$L(-z,k) = -L(z,-k), \tag{A12}$$

from which it immediately follows that

$$\int_{-1}^{1} dz L(z,0) = 0 \tag{A13}$$

and

$$\int_{-1}^{1} dz\,\frac{L(z,-k)}{\nu_+ + \frac{1}{2}k^2 - zk} = -\int_{-1}^{1} dz\,\frac{L(z,k)}{\nu_+ + \frac{1}{2}k^2 + zk}. \tag{A14}$$

Using (A14), (A10) can be rewritten

$$Q_0^2(kk_F, 2\nu E_F/\hbar) = \frac{2}{\pi^4 a_0^2 k_F^2 k^5}\int_{-1}^{1} dz[L(z,k) - L(z,0)]\left(\frac{1}{\nu_+ + \frac{1}{2}k^2 + zk} - \frac{1}{\nu_+ - \frac{1}{2}k^2 - zk}\right). \tag{A15}$$

Therefore,

$$\int_0^\infty d\nu\,\mathrm{Im}Q_0^2(kk_F, 2\nu E_F/\hbar) = -\frac{2\pi}{\pi^4 a_0^2 k_F^2 k^5}\int_{-1}^{1} dz[L(z,k) - L(z,0)]\int_0^\infty d\nu[\delta(\nu + \tfrac{1}{2}k^2 + zk) - \delta(\nu - \tfrac{1}{2}k^2 - zk)]. \tag{A16}$$

For $k>2$, the first δ function yields no contribution, while the second δ function contributes for all z under consideration. Because of (A13) we thus obtain

$$\int_0^\infty d\nu\,\mathrm{Im}Q_0^2(kk_F, 2\nu E_F/\hbar)$$
$$\underset{k>2}{=} \frac{2\pi}{\pi^4 a_0^2 k_F^2 k^5}\int d^3r \int d^3r' \mathfrak{N}(\vec{r})\mathfrak{N}(\vec{r}')\frac{1}{z - z' + k}, \tag{A17}$$

where the expression (A11) for $L(z,k)$ has been used again. In the limit of large k, the leading term in $1/k$ becomes

$$\int_0^\infty d\nu\,\mathrm{Im}Q_0^2(kk_F, 2\nu E_F/\hbar) \underset{k\to\infty}{\longrightarrow} \frac{32}{9\pi a_0^2 k_F^2}\frac{1}{k^6}. \tag{A18}$$

We now evaluate $\int_0^\infty d\nu\,\mathrm{Im}GQ_0$, starting from the result (38) of Paper I,

$$G(kk_F, 2\nu E_F/\hbar)Q_0^2(kk_F, 2\nu E_F/\hbar)$$
$$= \frac{1}{\pi^2 a_0^2 k_F^2 k^3}\int_{-1}^{1} dz\,\mathcal{T}(z,k)\left(\frac{1}{\nu_+ - \frac{1}{2}k^2 - kz} - \frac{1}{\nu_+ + \frac{1}{2}k^2 + kz}\right), \tag{A19}$$

where, from (36) of Paper I

$$\mathcal{T}(z,k) = [\mathfrak{F}(z,k) - \mathfrak{F}(z,0)] - [\mathfrak{K}(z,k) - \mathfrak{K}(z,0)], \tag{A20}$$

with $\mathfrak{F}(z,k)$ given by (34) of Paper I:

$$\mathfrak{F}(z,k)=-k\,\frac{1-(1+k^2+2zk)^{1/2}}{(1+k^2+2zk)^{1/2}}\ln\left|\frac{1+(1+k^2+2zk)^{1/2}}{1-(1+k^2+2zk)^{1/2}}\right|+(z+k)\frac{1-(z+k)^2}{[(z+k)^2]^{1/2}}\ln\left|\frac{1+[(z+k)^2]^{1/2}}{1-[(z+k)^2]^{1/2}}\right|. \tag{A21}$$

For $\mathcal{K}(z,k)$ we use an expression which is easily derived by combining (8), (15), (22), and (26) of Paper I:

$$\mathcal{K}(z,k)=\frac{1}{\pi^2}\int_{-1}^{1}dz'\int_0^{(1-z^2)^{1/2}}\rho\,d\rho\int_0^{(1-z'^2)^{1/2}}\rho'\,d\rho'\int_0^{2\pi}d\varphi\int_0^{2\pi}d\varphi'\,\frac{1}{z-z'+k}\times\frac{1}{\rho^2+\rho'^2+(z-z'+k)^2-2\rho\rho'\cos\varphi}. \tag{A22}$$

From the symmetry property, similar to (A13) but for $\mathcal{K}(z,k)$ and $\mathfrak{F}(z,k)$, it immediately follows that

$$\int_{-1}^{1}dz\mathcal{K}(z,0)=\int_{-1}^{1}dz\,\mathfrak{F}(z,0)=0. \tag{A23}$$

Next, defining

$$\mathcal{T}(t)\equiv\int d^3r\,\mathfrak{N}(\vec{r})\,\frac{1}{|\vec{r}-\vec{t}|}=2\pi\left(1+\frac{1-t^2}{2t}\ln\left|\frac{1+t}{1-t}\right|\right), \tag{A24}$$

one easily shows that

$$\mathfrak{F}(z,k)=2z-\frac{1}{2\pi}\frac{d}{dz}\int_{z^2+k^2+2zk}^{1+k^2+2zk}du\,\mathcal{T}(\sqrt{u}). \tag{A25}$$

Therefore, from an integration by parts, (A25) leads to

$$\int_{-1}^{1}dz\,\mathfrak{F}(z,k)=0, \tag{A26}$$

which is an exact result, valid for all k.

From (A22), it follows that

$$\int_{-1}^{1}dz\mathcal{K}(z,k)=\frac{1}{\pi^2}\int d^3r\int d^3r'\,\mathfrak{N}(\vec{r})\mathfrak{N}(\vec{r}')\times\frac{1}{z-z'+k}\,\frac{1}{|\vec{r}-\vec{r}'+\vec{k}|^2}, \tag{A27}$$

and the leading term in $1/k$ for very large k thus becomes

$$\int_{-1}^{1}dz\mathcal{K}(z,k)\xrightarrow[k\to\infty]{}\frac{16}{9}\frac{1}{k^3}. \tag{A28}$$

Using (A23), (A26), and (A28) the imaginary part of (A21), integrated over ν becomes

$$\int_0^\infty d\nu\,\mathrm{Im}G(kk_F,2\nu E_F/\hbar)Q_0^2(kk_F,2\nu E_F/\hbar)=-\frac{1}{\pi a_0^2k_F^2k^3}\int_{-1}^{1}dz\mathcal{T}(z,k)\times\int_0^\infty d\nu[\delta(\nu-\tfrac{1}{2}k^2-kz)-\delta(\nu+\tfrac{1}{2}k^2+kz)]. \tag{A29}$$

For $k>2$, the second δ function in (A29) yields no contribution and the first δ function contributes for any z under consideration. From (A20), and using (A23) and (A26), the term in $\mathcal{K}(z,k)$ survives, and the result of the integral is then given by (A28):

$$\int_0^\infty d\nu\,\mathrm{Im}G(kk_F,2\nu E_F/\hbar)Q_0^2(kk_F,2\nu E_F/\hbar)\xrightarrow[k\to\infty]{}\frac{16}{9\pi a_0^2k_F^2}\frac{1}{k^6}. \tag{A30}$$

Combining (A7), (A18), and (A30), an expansion of the integral (A3) for $S(kk_F)$ in powers of $(1/k)$ using (A2) leads to

$$S(kk_F)\xrightarrow[k\to\infty]{}1-\frac{4}{3\pi}\frac{1}{a_0k_F}\frac{1}{k^4}, \tag{A31}$$

which is precisely Eq. (13) of Sec. II.

*Work performed in the framework of the joint project E. S. I. S. (Electronic Structure in Solids) of the University of Antwerpen and the University of Liège.

‡Institute of Applied Mathematics, Rijksuniversitair Centrum Antwerpen, Groenenborgerlaan 171, B-2020 Antwerpen, Belgium.

[1]J. T. Devreese, F. Brosens, and L. F. Lemmens, Phys. Rev. B. 21, 1349 (1980), preceding paper.
[2]J. Hubbard, Proc. R. Soc. London, Ser. A 243, 336 (1957).
[3]D. R. Hamann and A. W. Overhauser, Phys. Rev. B 143, 183 (1966).
[4]P. E. Batson, C. H. Chen, and J. Silcox, Phys. Rev. Lett. 37, 937 (1976).
[5]D. Pines and P. Nozières, *The Theory of Quantum Liquids* (Benjamin, New York, 1966), Vol. 1, Chaps. 3–5.
[6]A. K. Rajagopal, Phys. Rev. A 6, 1239 (1972).
[7]F. Brosens, L. F. Lemmens, and J. T. Devreese, Phys. Status Solidi B 74, 45 (1976).
[8]D. N. Tripathy and S. S. Mandal, Phys. Rev. B 16, 231 (1977).
[9]L. J. Sham, Phys. Rev. B 7, 4357 (1973).
[10]G. Niklasson, Phys. Rev. B 10, 3052 (1974).
[11]F. Toigo and T. O. Woodruff, Phys. Rev. B 2, 3958

(1970); 4, 371 (1971).
[12]D. J. W. Geldart, R. Taylor, and M. Rasolt, Phys. Rev. B 5, 2740 (1972).
[13]J. C. Kimball, Phys. Rev. A 7, 1648 (1973); Phys. Rev. B 14, 2371 (1976).
[14]P. Nozières and D. Pines, Nuovo Cimento 9, 470 (1958).
[15]R. W. Shaw Jr., J. Phys. C 3, 1140 (1970).
[16]F. Brosens, L. F. Lemmens, and J. T. Devreese, Phys. Status Solidi B 82, 117 (1977).
[17]A. A. Kugler, J. Stat. Phys. 12, 35 (1975).
[18]F. Brosens, L. F. Lemmens, and J. T. Devreese, Phys. Status Solidi B 81, 551 (1977).
[19]A. W. Overhauser, Adv. Phys. 27, 343 (1978).
[20]F. Brosens, J. T. Devreese, and L. F. Lemmens, Phys. Status Solidi B 80, 99 (1977).
[21]J. T. Devreese, F. Brosens, and L. F. Lemmens, Phys. Status Solidi B 91, 349 (1979).
[22]P. Vashishta and K. S. Singwi, Phys. Rev. B 6, 875 (1972).
[23]E. P. Wigner, Trans. Fara. Soc. 34, 678 (1938).
[24]N. Wiser and M. M. Cohen, J. Phys. C 2, 193 (1969).
[25]A. W. Overhauser, Phys. Rev. 128, 1437 (1962).